IMAGING AND MONITORING THE PARSEC-SCALE JET IN 3C 273 WITH THE VSOP MISSION

A. P. Lobanov[1], J. A. Zensus[1], Z. Abraham[2], E. Carrara[2], and S. C. Unwin[3]

[1] *Max-Planck-Institut für Radioastronomie, Auf dem Hügel 69, D–53121 Bonn, Germany*
[2] *University of Saõ Paulo, Brazil*
[3] *Jet Propulsion Laboratory, Pasadena, USA*

ABSTRACT

We present results from the first observing epoch (December 1997) of 5 GHz VSOP monitoring program of the parsec–scale jet in 3C 273. At the resolution achieved by the VSOP observation, the jet is transversely resolved, and it exhibits significant edge brightening. The latter may result from velocity gradients or reacceleration zones existing in the jet, due to interactions between the faster jet plasma and slower, non-relativistic outflow or ambient medium.

VSOP Monitoring of Parsec-Scale Jet in 3C 273

Monitoring of the quasar 3C 273 is a key-science program of the VSOP mission aimed at obtaining a sequence of high linear resolution images of the parsec-scale jet in this object and studying transverse structure of relativistic outflows from the AGN. At kiloparsec scales, the jet profile in 3C 273 can be decomposed into two components corresponding to a fast, collimated beam surrounded by a wide cocoon (Conway *et al.* 1993). The cocoon can be produced by entrainment of a non-relativistic material surrounding the highly relativistic core of the jet and subsequent dissipation of the entrained material. By measuring the relative representation of these two components in the parsec-scale jet, one can estimate the degree of entrainment and degree of interaction between the jet and ambient medium. Here we discuss the first epoch of the VSOP monitoring of 3C 273, and present an image in which the jet is transversely resolved and shows evidence for possible velocity gradients and beam-cocoon type of morphology.

Observations and Images

3C 273 was observed with the VSOP on December 22 1997, with the HALCA satellite radio telescope (Hirabayashi 1996), 11 ground telescopes (Effelsberg and 10 VLBA antennas) and two Satellite Tracking Stations (Robledo and Green Bank) participating in the observation. The data were recorded at 4.8 GHz, with a 32 MHz bandwidth divided into 256 spectral channels. The correlation was done at the VLBA correlator in Socorro. The fringe fitting and imaging were done using AIPS and DIFMAP (Shepherd *et al.* 1994) packages. For brevity, we omit here the details of the fringe-fitting, and will discuss them elsewhere (Lobanov *et al.*, in prep.). The resulting *uv*-coverage and visibility distribution are shown in Figure 1.

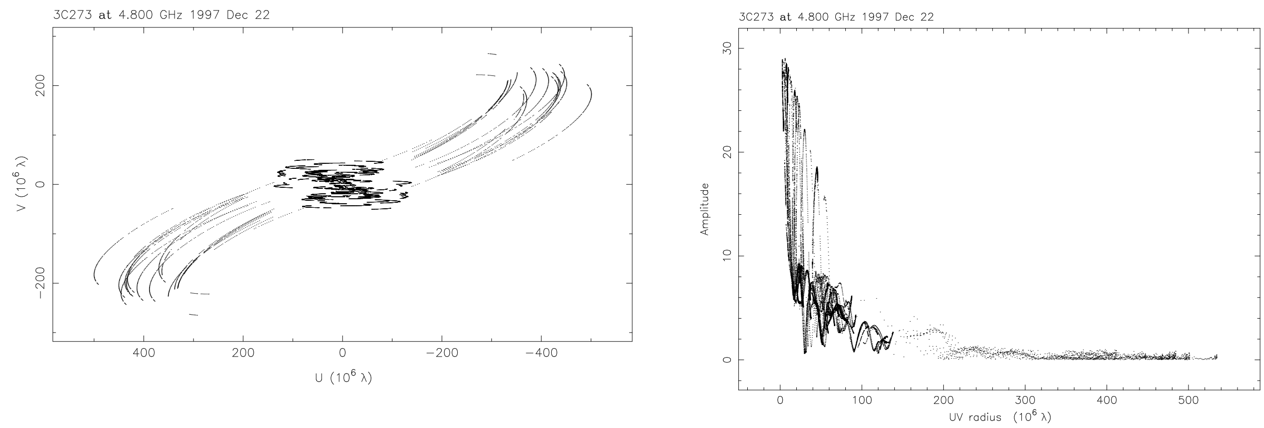

Figure 1: VSOP observation of 3C 273. Left panel: *uv*-coverage; right panel: visibility distribution. The space baselines cover the range of *uv*-spacings between 140 Mλ and 540 Mλ.

Table 1: Parameters of the images

Image (1)	$S_{\rm tot}$ (2)	$S_{\rm max}$ (3)	$S_{\rm min}$ (4)	$\sigma_{\rm RMS}$ (5)	$D_{\rm rms}^{\rm peak}$ (6)
VLBI	28.66	5.38	-0.008	1.1	4500:1
VSOP	28.33	4.52	-0.019	2.1	2100:1

Column designation: 2 – total CLEAN flux [Jy]; 3 – peak flux density [Jy/beam]; 4 – lowest negative flux density [Jy/beam]; 5 – RMS noise [mJy/beam]; 6 – peak-to-RMS dynamic range.

From the fringe-fitted data we obtained two images: an image with only the ground baseline data (left panel of Figure 2: the VLBI image hereafter) and an image from the entire dataset (right panel in Figure 2: the VSOP image hereafter). We use natural weighting for producing both images, enhancing the sensitivity to extended emission at the price of slightly decreased image resolution. The gridding weights are also scaled by amplitude errors raised to the power of -1. Both phase self-calibration and overall gain scaling have been used, with the antenna gains being allowed to vary only after the total model flux has approached the zero spacing flux to within 3%. The main characteristics of the images are summarized in Table 1. We would like to emphasize the excellent data quality which has resulted in high-dynamic ranges reached both in the ground VLBI and VSOP images.

Discussion

The VSOP image in Figure 2 shows remarkable deviations of transverse emission distribution from a Gaussian shape, owing to the favorable orientations of the space baselines which provide a 0.7 mas resolution in the direction perpendicular to the jet axis. This is particularly visible in the profiles taken across the jet (Figure 3). Possible confusion due to sidelobe effects is ruled out by the closure phase fits: the fits show significant deterioration, if the regions on the edges of the jet are excluded.

The ground VLBI image also resolves the jet transversely, and suggests possible edge brightening (similar to the high dynamic range ground VLBI images at 1.6 GHz, Unwin *et al.* 1994). However, only with the improved resolution of the VSOP image, it becomes possible to assess the true complexity of the transverse structure of the jet, with up to three emission components across the jet (panel B in Figure 3). The stronger

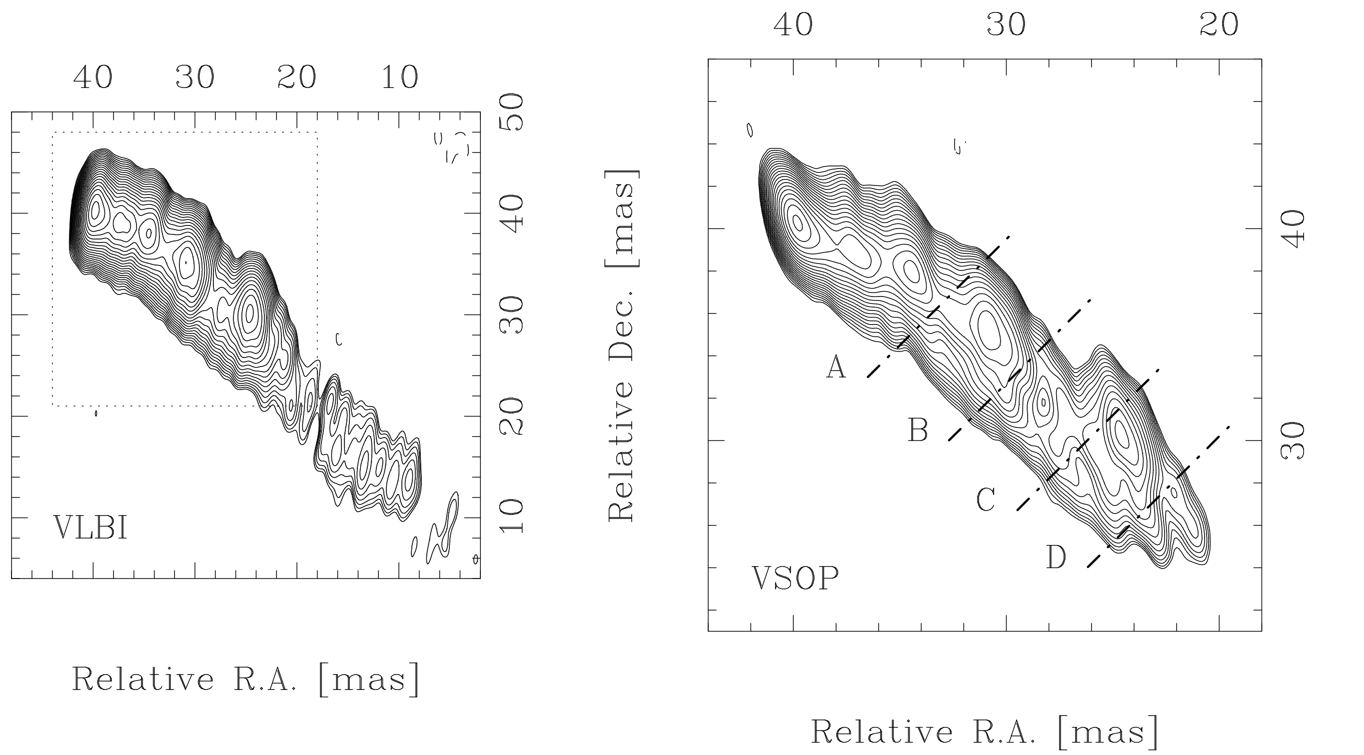

Figure 2: Naturally weighted ground array (left) and VSOP (right) images of 3C 273. The image parameters are as follows. The ground array image: restoring beam is 3.73×1.13 mas at P.A.= −10.27 deg; contour levels are drawn at 3.7×(-1, 1, 1.41, 2, ..., 1024) mJy/beam; the peak flux density is 5.38 Jy/beam. The VSOP image: restoring beam is 2.09×0.70 mas at P.A.= 12.9 deg; contour levels are drawn at 4.1×(-1, 1, 1.41, 2, ..., 1024) mJy/beam; the peak flux density is 4.52 Jy/beam. Dot-dashed lines denote the locations of the flux density profiles shown in Figure 3.

central component often dominates the profiles, possibly masking the presence of the third emitting feature. One can speculate that the stronger central component is produced by a shocked plasma embedded in an underlying flow with Kelvin-Helmholtz instabilities revealed in the two weaker emission components and the observed slight curvature of the jet. The helical morphology of underlying emission is also suggested by the larger scale structures seen in the ground VLBI image. The embedded, brighter features do not appear following the same curved path, but rather tend to drift closer to the northern edge of the jet, with increasing distance. This may reflect their possible ballistic trajectories reported earlier (Abraham *et al.*, 1996). The subsequent VSOP observations should provide a better basis for making conclusions on this issue. Measuring the relative strength of the weaker emission features across the jet should also allow to determine whether the helical or elliptical instability modes dominate the underlying plasma. Another possibility that can be further explored with the VSOP monitoring is the role of entrainment in the formation of the weaker emission features and the relation between the parsec-scale and kiloparsec-scale jet in 3C 273.

Conclusions

We have presented a high resolution and high dynamic range image obtained from the first epoch of the monitoring of 3C 273 with teh VSOP at 5 GHz. The improved resolution and favorable orientation of the space baselines have allowed to resolve the transverse structure of the parsec-scale jet. In the obtained VSOP image, the jet appears to contain several emitting components possibly related to shocks and plasma instabilities both exisiting in the jet. Further VSOP monitoring would provide an essential information for determining the nature of the individual emitting components.

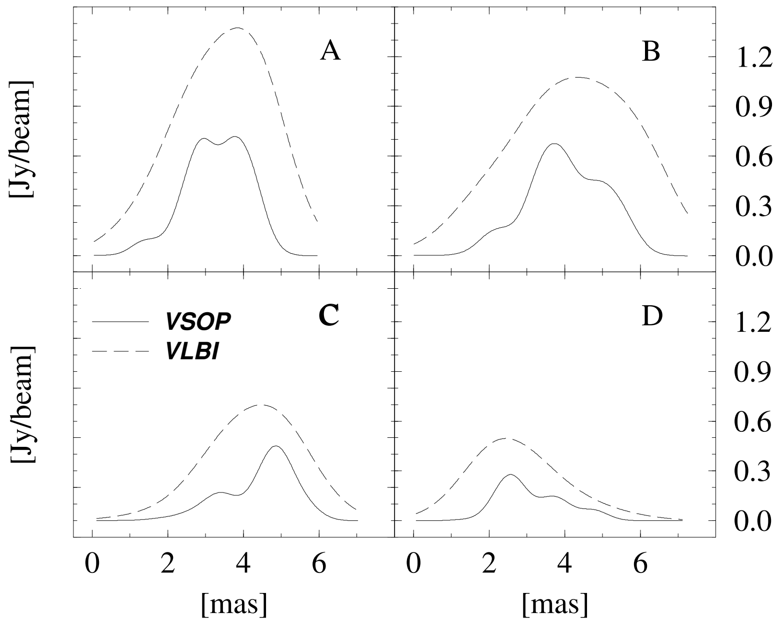

Figure 3: Flux density profiles across the jet in the VSOP (solid lines) and VLBA (dashed lines) images. The locations of the profiles are shown in the right panel of Figure 2.

Acknowledgments

We gratefully acknowledge the VSOP Project, which is led by the Japanese Institute of Space and Astronautical Science in cooperation with many organizations and radio telescopes around the world. We thank D. Graham for technical support at Effelsberg. The National Radio Astronomy Observatory is a facility of the National Science Foundation operated under cooperative agreement by Associated Universities, Inc.

References

Abraham, Z., Carrara, E., Zensus, J. A., and Unwin, S.C., *A&AS*, **115**, 543 (1996).

Conway R. G., *et al.*, *A&A*, **267**, 347 (1993).

Hirabayashi, H., *Springer Science (Quarterly)*,**2**, 11, 6 (1996).

Shepherd M. C., Pearson, T. J., and Taylor, G. B., *BAAS*, **26**, 987 (1994).

Unwin, S. C., Davis, R. J., and Muxlow, T. W. B., p.81 in *Compact Extragalactic Radio Sources*, eds. J. A. Zensus and K .I. Kellermann, NRAO, Socorro (1994).